JOURNAL OF CATALYSIS 86, 95–107 (1984)

CO Hydrogenation with Alumina-Supported Catalysts Prepared from $[Os(CO)_5]$

E. O. ODEBUNMI,*,[1] Y. ZHAO,†,[2] H. KNÖZINGER,†,[3] B. TESCHE,‡ W. H. MANOGUE,*,§ B. C. GATES,* AND J. HULSE†

*Center for Catalytic Science and Technology, Department of Chemical Engineering, University of Delaware, Newark, Delaware 19711, †Institut für Physikalische Chemie, Universität München, Sophienstrasse 11, 8000 München 2, Federal Republic of Germany, ‡Fritz-Haber-Institut der Max-Planck-Gesellschaft, Faraday-Weg 4-6, 1000 Berlin 33, Federal Republic of Germany, and §E. I. DuPont de Nemours and Co., Experimental Station, Wilmington, Delaware 19898

Received August 4, 1983; revised September 20, 1983

γ-Al_2O_3-supported osmium was prepared from $[Os(CO)_5]$ and characterized by infrared spectroscopy and transmission electron microscopy before and after use in catalytic hydrogenation of CO at 1 or 10 bar and 523–598 K. Mononuclear osmium carbonyl complexes were formed initially on the Al_2O_3 surface, and when the samples were brought in contact with H_2, the osmium was reduced, forming small metal aggregates. Samples were reduced either severely (in 10 bar of H_2 for 10 h), giving large aggregates, or mildly (in 1 bar of H_2 for 1 h), giving smaller aggregates. The properties of the catalysts for CO hydrogenation were compared with those of samples prepared from $[H_2OsCl_6]$ and $[Os_3(CO)_{12}]$, which consisted of mononuclear osmium complexes and ensembles consisting of three or fewer osmium ions. The activities of the latter catalysts for hydrocarbon formation and the chain growth probabilities were significantly less than those of the catalysts containing Os aggregates. The chain growth probability and the olefin : paraffin ratios were greater for the larger aggregates. Surface intermediates are suggested involving bifunctional interactions of CO with Os metal (or Os ion) sites and neighboring Al^{3+} sites.

INTRODUCTION

Product distributions in CO hydrogenation are strongly dependent on the nature of the metal catalyst (*1*) and the support (*2*). Catalytic properties of a given metal/support combination may also be influenced by the structure of the metal precursor. This dependence may result from (i) the formation of different active species from different precursors (e.g., metal ions vs metal particles); (ii) different metal particle sizes; and (iii) modifications of the support surface [e.g., chlorine incorporation onto the surface when metal chlorides are used as precursors (*3*)].

It has been suggested that CO hydrogenation reactions involving C–O bond scission (dissociative chemisorption) and C–C bond formation require catalysts with neighboring metal centers, i.e., surfaces or metal clusters (*4*). It has also been suggested that the length of the growing hydrocarbon chain is sensitive to the number of accessible metal centers on the surface of a metal particle or cluster: data obtained with Ru aggregates encaged in zeolites showed a cut-off in chain length near C_2, C_6, or C_{11}, depending on the size of the zeolite cage, which determined the size of the Ru aggregates (*5*).

Supported catalysts prepared from metal clusters have been found to give unusual selectivities in CO hydrogenation (*2, 6*). In an investigation of these materials, we reported CO hydrogenation activity of alumina-supported catalysts derived from $[Os_3(CO)_{12}]$, $[H_4Os_4(CO)_{12}]$, and $[H_2OsCl_6]$

[1] Present address: Chemistry Department, University of Ilorin, Ilorin, Nigeria.

[2] Present address: Dalian Institute of Chemical Physics, Chinese Academy of Sciences, Dalian, People's Republic of China.

[3] To whom correspondence should be addressed.

0021-9517/84 $3.00

(*1, 3*) The results indicated the importance of precursor nuclearity in catalyst performance, although the data are too few to establish clear patterns

Regarding the CO activation step, an alternative to dissociative chemisorption on two neighboring metal centers has been advocated, which involves Lewis acid-induced reduction of CO (*8–10*) In this step, neighboring metal centers would not be required, since CO could be coordinated to a single metal site (an isolated atom or complex or an edge atom of a particle) and simultaneously interact with a Lewis acid site (e g , Al^{3+}_{cus}) through the carbonyl oxygen Infrared spectroscopy of adsorbed group VIb metal carbonyls has revealed evidence for this type of interaction (*11, 12*) Moreover, Cl^- incorporation into the Al_2O_3 support surface—which strongly enhances the Lewis acidity—appeared to increase the rate of methanation on the supported osmium catalysts mentioned above (*3*)

In continuing this research, we have now used the mononuclear osmium carbonyl $[Os(CO)_5]$ as a catalyst precursor The preparation with a metal carbonyl ensures the absence of modified surface properties of the support such as those mentioned above, and the mononuclear carbonyl precursor might be expected to permit the formation of isolated surface carbonyls Several investigations with group VIb carbonyls have demonstrated the formation of mononuclear tricarbonyl species on Al_2O_3 supports (*12–14*) The goal of this work was to characterize the structures of $[Os(CO)_5]$-derived catalysts and to determine their behavior for hydrogenation of CO The results were to be compared with those obtained previously with $[Os_3(CO)_{12}]$- and $[H_2OsCl_6]$-derived catalysts (*3*) in an attempt to determine relations between structures of the active species and catalytic activities and selectivities

EXPERIMENTAL METHODS

Materials and catalyst preparation The γ-Al_2O_3 used as a support was type P 110 C 1 from Degussa, which had a N_2 BET surface area of 100 $m^2\ g^{-1}$ $[Os(CO)_5]$ was synthesized according to literature methods (*15, 16*) One gram of OsO_4 (Merck) dissolved in 50 cm^3 of heptane was heated at 430 K in an autoclave under a CO partial pressure of 200 bar for 8 h The autoclave was then cooled to room temperature and brought to atmospheric pressure within 1 h The volatile $[Os(CO)_5]$ was then condensed into a trap kept at dry ice temperature

The Al_2O_3 support was heated in oxygen at 670 K and then evacuated ($<10^{-3}$ bar) at the same temperature prior to being brought in contact with a heptane solution of $[Os(CO)_5]$ under N_2 at dry ice temperature After warming to room temperature and removal of the supernatant solution, the material was dried by evacuation at room temperature and stored under N_2 Contact with air, however, could not be avoided during pressing of wafers for infrared spectroscopy and during loading of catalyst into the reactor

The catalyst contained 0 36 wt% Os, as determined by Analytische Laboratorien, Engelskirchen, FRG For comparison, the catalysts prepared from $[Os_3(CO)_{12}]$ and $[H_2OsCl_6]$ contained 0 34 and 1 18 wt% Os, respectively, their preparation and characterization were described previously (*3*)

Infrared spectroscopy Thin self-supporting wafers were pressed and placed in a previously described (*17*) transmission infrared cell permitting *in situ* heat treatment and chemisorption experiments The spectra were recorded on a Perkin-Elmer 225 spectrophotometer To reduce heat effects induced by the infrared beam, the Globar light source was run at only about 20% of its maximum power The spectral slit width in the carbonyl stretching region was typically 3 cm^{-1}

Some infrared spectra were also recorded with a Nicolet 7199 FTIR spectrometer The procedure and cells are described elsewhere (*18*)

Transmission electron microscopy In preparation for high-resolution transmis-

sion electron microscopy (TEM), the catalyst powder was ground and suspended in hexane A drop of the suspension was placed on a 4-nm carbon film mounted on a 1000 mesh Cu grid, and the hexane was allowed to evaporate

The micrographs were obtained with a Philips EM 400T microscope with an instrumental magnification of 360,000× and an acceleration voltage of 120 keV To improve the contrast, the objective aperture was reduced to ca 30 μm, which led to a restriction of the spatial frequency spectrum in the electron microscopic image and a restriction of the phase contrast to ≤0 3 nm

Catalytic reaction rate measurements The catalytic reaction experiments were carried out with a steady-state differential flow reactor, described elsewhere (*19*) About 2 g of catalyst powder was loaded into the copper-lined tubular reactor and held in place with glass wool plugs at inlet and outlet The reactor was purged thoroughly with helium and brought to pressure with hydrogen, the temperature was gradually raised to 548 K The catalyst pretreatment involved heating in hydrogen at 1 or 10 bar Subsequent catalyst reactivations (at the end of each experiment) involved treatment with flowing hydrogen at 548 K and the pressure of the following experiment for several hours This procedure completely restored catalyst activity and ensured the attainment of reproducible results

The hydrogenation of CO was investigated at pressures of 1 and 10 bar, temperatures, of 520 to 600 K, and various reactant compositions and flow rates The reactor effluent flowed through an on-line gas-sampling valve, and samples were periodically intercepted and injected into an Antek 300 gas chromatograph equipped with a flame-ionization detector Hydrocarbons were separated with an alumina column and oxygenates with a SE-30 column, each column was stainless steel, $\frac{1}{8}$ in in diameter and 6 ft in length

With temperature, pressure, and reactant gas flow rate held constant during an experiment, conversions of CO and hydrogen were measured as a function of time on stream For most experiments, steady-state conversion was obtained after about 20 h on stream The pure alumina support was inactive for CO hydrogenation

RESULTS AND DISCUSSION

Characterization of Unused Catalyst

A fresh wafer of catalyst prepared from $[Os(CO)_5]$ and γ-Al_2O_3 had bands in the carbonyl stretching region at 2125, 2098, 2035, and 1953 cm^{-1} (Fig 1, spectrum 1) This

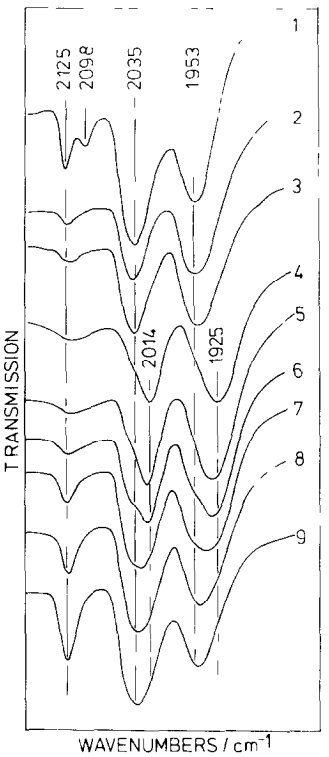

FIG 1 Infrared spectra of the unused catalyst prepared from $[Os(CO)_5]$ and γ-Al_2O_3 catalyst after various *in situ* treatments (1) "Fresh" catalyst after evacuation for 30 min at room temperature, (2) after treatment in H_2 (0 92 bar) at 473 K for 3 h, (3) at 473 K for 4 h, (4) at 573 K for 2 h, (5) after subsequent exposure of catalyst to CO (0 13 bar) at 373 K for 2 h, (6) at 423 K for 2 h, (7) at 473 K for 2 h, (8) at 523 K for 2 h, (9) at 573 K for 2 h Spectra were recorded at beam temperature

spectrum is probably a composite indicating the existence of more than one osmium carbonyl species on the γ-Al_2O_3 surface The three bands at 2125, 2035, and 1953 cm^{-1} are very close to those observed in the samples prepared from $[Os_3(CO)_{12}]$ and γ-Al_2O_3 and are attributed to a mixture of mononuclear $Os^{2+}(CO)_2$ and $Os^{2+}(CO)_3$ surface complexes (*3, 5, 20–22*) [4] Evacuation or treatment in hydrogen at temperatures <470 K eliminated the band at 2098 cm^{-1} and reduced the band at 2125 cm^{-1}, the two low-frequency bands remained close to their original positions (Fig 1, spectra 2 and 3) This behavior is also known from the samples prepared from $[Os_3(CO)_{12}]$ and γ-Al_2O_3 (*3, 5, 20*) and suggests a decarbonylation of the surface complexes to yield preferentially the dicarbonyl species $Os^{2+}(CO)_2$

Treatment of the sample in hydrogen at 573 K (Fig 1, spectrum 4) shifted the two bands to lower frequencies (2014 and 1925 cm^{-1}) with only a slight asymmetry remaining at the original band positions This trend is indicative of a reduction of the osmium species to a lower oxidation state (*3*) Subsequent exposure of the sample to a CO atmosphere at increasing temperatures reversed the frequency shift (Fig 1, spectra 5–9), the original spectrum was restored after treatment at 573 K in CO, suggesting reoxidation and recarbonylation of the osmium species We infer that at intermediate stages (e g , Fig 1, spectrum 6), there were at least two surface osmium complexes, one with Os in the +2 and one with Os in a lower oxidation state, with various degrees of carbonylation (di- and tri-carbonyls) This inference is confirmed by the superposition of three band pairs at 2125 and 2035 cm^{-1} $[Os^{2+}(CO)_3]$, 2035 and 1950 cm^{-1} $[Os^{2+}(CO)_2]$, at 2014 and 1925 cm^{-1} $[Os^{(2-x)+}(CO)_2]$ The existence of Os^+ in reduced samples has recently been demonstrated by ESR (*23*)

[4] An alternative interpretation has been offered for a similar 3-band spectrum for supported catalysts prepared from osmium carbonyls in a different way (*31*)

As suggested previously for $Os_3(CO)_{12}$ (*3, 20*), we assume that the oxidation of Os occurs due to reaction of $Os(CO)_5$ with the Al_2O_3 surface, although we cannot completely rule out the possible role of traces of oxygen

In summary, the infrared spectra suggest the formation of mononuclear surface osmium carbonyl complexes, and there is no indication of aggregation of the metal under the conditions of the experiments

The samples were also investigated by TEM, with typical results shown in Figs 2a and b Lattice planes of the γ-Al_2O_3 support are clearly evident, indicating the resolution obtained, no scattering centers in the size range >1 nm were detected in any of the micrographs, even after hydrogen treatment of the sample The micrographs therefore confirm the conclusion that aggregation of the surface osmium did not occur under the conditions of the infrared investigations We recall that scattering centers of size $\lesssim$1 nm were observed in samples prepared from $[Os_3(CO)_{12}]$ and γ-Al_2O_3, they were attributed to ensembles consisting of three Os atoms each (*3, 24*) This interpretation was confirmed by TEM investigations of $[Os_3(CO)_{12}]$ supported on well-defined self-supporting Al_2O_3 films (*25*)

We recognize that the interpretation of micrographs of dispersed powder samples may be misleading because such samples present variable layer thicknesses and, consequently, varying degrees of defocusing, which may produce contrasts which are susceptible to misinterpretation as real structures Since no contrast in the size range of 1 nm was found in the micrographs—and since scattering centers all the same size were observed in the similar samples prepared from $[Os_3(CO)_{12}]$ and γ-Al_2O_3—we conclude that aggregates about 1 nm in size would have been detected if they had been present in the samples prepared from $[Os(CO)_5]$ and γ-Al_2O_3

Catalytic Hydrogenation of CO

The freshly prepared catalyst derived

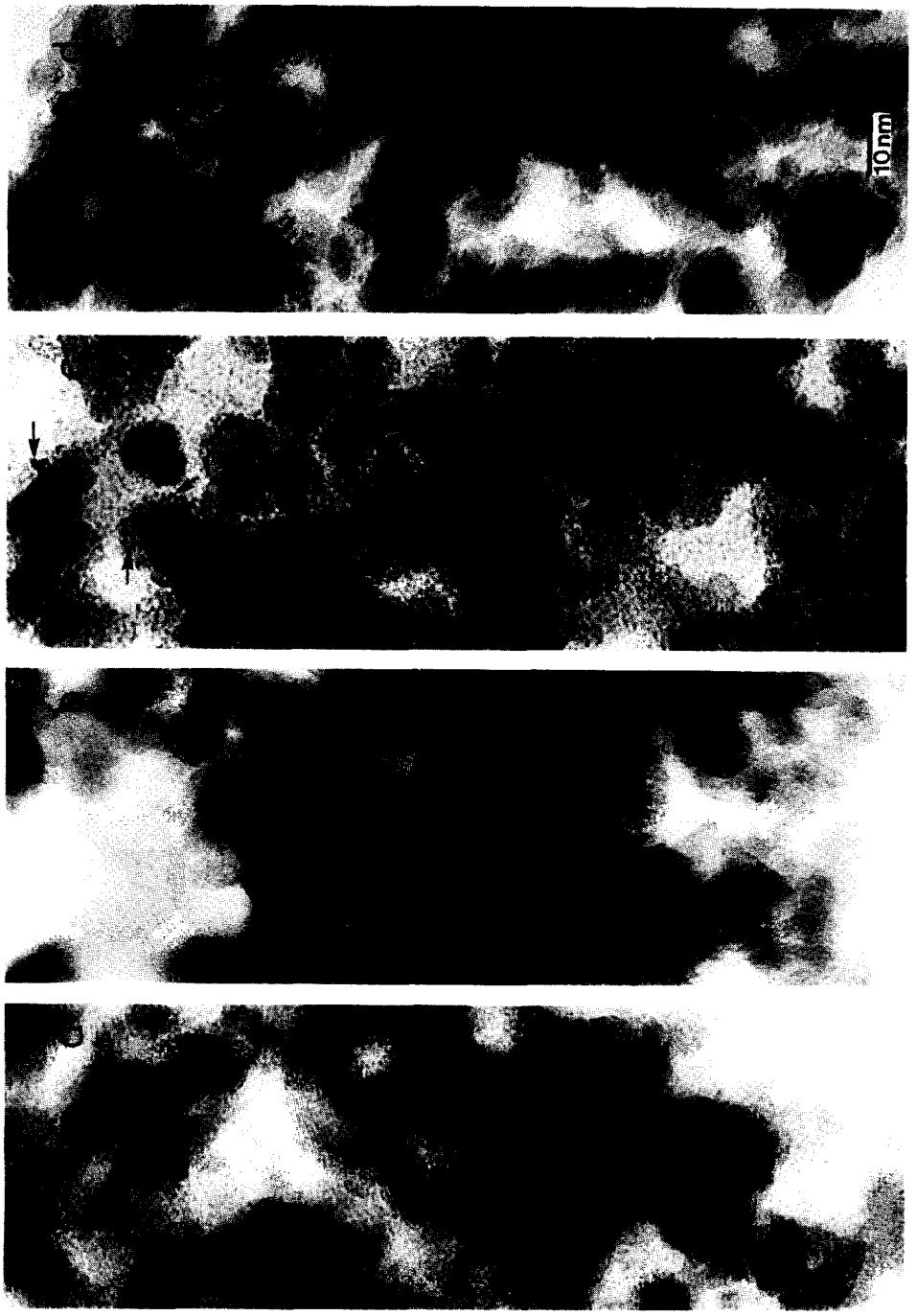

FIG. 2. Transmission electron micrographs of $[Os(CO)_5]$-derived catalysts: (a) freshly prepared; (b) same after reduction in H_2 [sample corresponds to ir wafer of Fig. 1 after treatments (1)–(9)]; (c) $[Os(CO)_5]/\gamma\text{-}Al_2O_3$, after treatment B and use as a catalyst; (d) $[Os(CO)_5]/\gamma\text{-}Al_2O_3$, after treatment A and use as a catalyst.

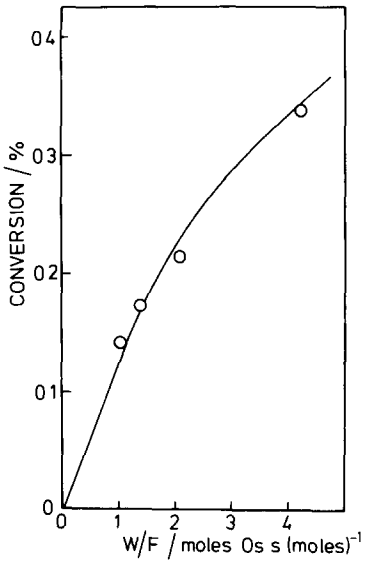

FIG 3 Conversion of CO + H_2 into hydrocarbons in the presence of a catalyst prepared from $[Os(CO)_5]$ and γ-Al_2O_3 (treatment A) (reaction temperature, 548 K, H_2 CO molar ratio, 1 1, total pressure, 10 bar)

from $[Os(CO)_5]$ was pretreated under two different sets of conditions prior to its use in CO hydrogenation The relatively severe treatment A [catalyst $[Os(CO)_5]$-A] consisted of exposure of the sample to flowing H_2 at a pressure of 10 bar at 548 K for approximately 10 h In contrast, in the relatively mild treatment B [catalyst $[Os(CO)_5]$-B], the sample was exposed to flowing H_2 at a pressure of only 1 bar for 1 h at the same temperature Most of the catalytic reaction experiments were carried out with a catalyst treated by procedure A

A typical plot of the conversion of CO + H_2 to hydrocarbons versus inverse space velocity is shown in Fig 3 These plots gave straight lines passing through the origin with curvature at the higher conversions Reaction rates were calculated from data collected within the linear portions of these plots A summary of the catalytic reaction rate data is given in Tables 1 and 2

Hydrocarbons (C_1 through C_6) were the main products of the catalytic reaction Oxygenates were formed in almost negligible amounts, dimethyl ether being about 1% of the products observed with the freshly reduced catalyst (We infer that the ether formed from catalytic dehydration of methanol on acidic sites of the Al_2O_3 which is known to be active for this reaction (*34*)) Oxygenate formation declined as the catalyst aged, the ether was typically <0 2% of the products for the data recorded here

Methane was the predominant product and amounted to 72% of the hydrocarbon formed at 523 K and 10 bar with a feed molar ratio H_2 CO = 1 1 As the reaction temperature increased, the selectivity to methane decreased (to 37% at 598 K) and

TABLE 1

Temperature Dependence of CO Hydrogenation Catalyzed by γ-Al_2O_3-Supported Os Prepared from $[Os(CO)_5]$ (Pretreatment A)[a]

Temperature (K)	Percentage conversion	$10^4 r_{\Sigma HC}$[b]	$10^4 r_{CH_4}$[b]	Selectivities[c]				Schulz–Flory parameter, α[d]
				$\frac{C_1}{\Sigma HC}$	$\frac{C_2}{\Sigma HC}$	$\frac{C_3}{\Sigma HC}$	$\frac{C_4}{\Sigma HC}$	
523	0 11	5 2	3 8	0 72	0 16	0 07	0 04	1 03
548	0 22	10 1	6 3	0 62	0 22	0 10	0 04	0 98
573	0 43	20 0	9 3	0 47	0 25	0 16	0 08	0 81
598	0 80	37 7	13 9	0 37	0 23	0 22	0 11	0 65

[a] Reaction conditions pressure = 10 bar, H_2 CO = 1 1 (20 cm^3/min total flow)

[b] Rate r of hydrocarbon (or methane) formation, mol (mol of Os s)$^{-1}$

[c] Rate of formation of species i divided by total rate of hydrocarbon formation ($C_1 = CH_4$ $C_2 = C_2H_6 + C_2H_4$, etc)

[d] The mean errors of α are ±0 05

TABLE 2

Effects of Total Pressure, H_2 CO Molar Ratio and Temperature on Product Distributions in CO Hydrogenation Catalyzed by γ-Al_2O_3-Supported Os Prepared from $[Os(CO)_5]$ (Pretreatment A)

Temperature (K)	H_2 CO molar ratio	Pressure (bar)	Percentage conversion	Activity		Selectivity						Olefin paraffin ratio				
				$10^4 r_{\Sigma HC}$[a]	$10^4 r_{CH_4}$[b]	$\frac{C_1}{\Sigma HC}$	$\frac{C_2}{\Sigma HC}$	$\frac{C_3}{\Sigma HC}$	$\frac{C_4}{\Sigma HC}$	$\frac{C_5}{\Sigma HC}$	$\frac{C_6}{\Sigma HC}$	$\frac{C_2H_4}{C_2H_6}$	$\frac{C_3H_6}{C_3H_8}$	$\frac{C_4H_8}{C_4H_{10}}$	$\frac{C_5H_{10}}{C_5H_{12}}$	$\frac{C_6H_{12}}{C_6H_{14}}$
548	1	10	0 22	10 1	6 3	0 62	0 22	0 10	0 04	0 01	—	0 31	1 05	1 33	0 86	0 44
548	3	10	0 30	28 5	19 4	0 68	0 20	0 08	0 03	0 01	—	0 2	0 89	1 14	0 56	0 23
598	1	10	0 80	37 7	13 9	0 37	0 23	0 22	0 11	0 04	0 02	0 65	1 22	1 73	1 49	1 06
598	3	10	1 18	111 1	48 9	0 44	0 22	0 21	0 04	0 03	0 01	0 26	0 86	1 08	0 67	0 42
548	1	1	0 14	6 6	4 9	0 74	0 15	0 07	0 03	0 01	—	0 63	1 61	1 45	1 05	0 98
548	3	1	0 12	11 5	8 9	0 78	0 14	0 06	0 01	0 01	—	0 49	1 31	1 00	0 58	0 56
598	1	1	0 44	20 7	9 7	0 47	0 28	0 16	0 06	0 02	0 01	0 87	3 15	3 14	2 19	1 26
598	3	1	0 79	74 2	38 6	0 52	0 25	0 15	0 05	0 02	0 01	0 40	1 87	1 94	1 45	0 80

[a] Rate r of formation of all hydrocarbons

[b] Rate r of formation of methane mol (mol of Os s)$^{-1}$

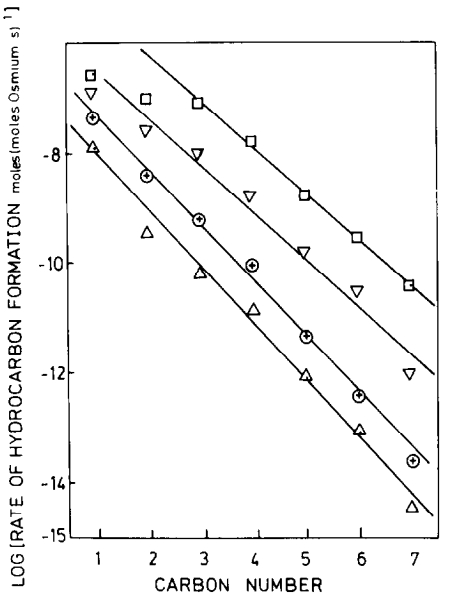

FIG 4 Schulz–Flory product distributions for reaction temperatures of 523 K (Δ), 548 K (○), 573 K (▽), and 598 K (□) Reaction conditions are as given in Table 1

the selectivity to higher hydrocarbons increased (Table 1) The selectivity to methane decreased as the contact time was increased at constant temperature and pressure, and the rate of formation of other hydrocarbons (particularly C_2 and C_3) appeared to increase The apparent activation energy of the CO + H_2 reaction was obtained from Arrhenius plots for the total rate of hydrocarbon formation, the value is 66 kJ mol^{-1}

The effects of pressure and feed gas composition on conversion and product selectivity are illustrated by the data of Table 2 As the pressure increased, the total conversion to hydrocarbons increased, and the selectivity to methane and the ratio of olefins to paraffins both decreased The olefin paraffin ratio for C_2 through C_5 also increased slightly as the reaction temperature increased

The feed ratio of H_2 to CO had a significant effect on product distribution As this ratio increased, the conversion to hydrocarbons increased markedly (Table 2) The selectivity to C_1, C_2, C_3, etc hydrocarbons appeared to be only little affected However, olefin paraffin ratios decreased significantly with increasing H_2 CO ratios at all the pressures and temperatures applied, consistent with the occurrence of olefin hydrogenation The activity of these catalysts for ethylene hydrogenation was tested in independent experiments

The distributions of hydrocarbon products conformed to the Schulz–Flory distribution at all the observed temperatures, as shown in Fig 4 Deviations from a straight line were observed only for C_1 and C_2 at the highest temperatures (573 and 598 K) The slopes of the straight lines determine the chain growth probability, α, and these values are summarized in Table 1, the value of α decreased as reaction temperature increased

The olefin paraffin ratio passed through a maximum for C_4 hydrocarbons when the pressure was 10 bar (Table 2, Fig 5) This maximum was shifted to C_3 hydrocarbons at the lower pressure (1 bar) The position of the maximum olefin paraffin ratio, how-

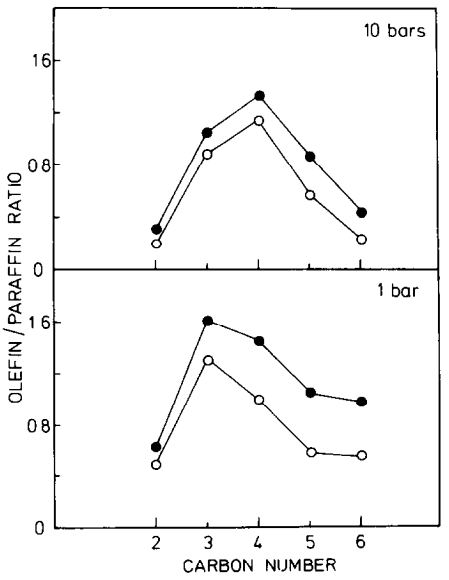

FIG 5 Olefin paraffin ratios for C_2 through C_6 hydrocarbons at 548 K and 10 and 1 bar total pressure and H_2 CO ratios of 1 1 (●) and 3 1 (○)

TABLE 3

CO Hydrogenation on $[Os(CO)_5]$-Derived Catalysts at 548 K[a]

	Catalyst	
	$[Os(CO)_5]$-A[c]	$[Os(CO)_5]$-B
$10^4 r_{\Sigma HC}$[b]	10 40	2 54
$10^4 r_{CH_4}$[b]	7 31	1 72
Selectivity		
(C_1 ΣHC)	0 72	0 68
(C_2 ΣHC)	0 16	0 24
(C_3 ΣHC)	0 07	0 06
(C_4 ΣHC)	0 04	0 02
(C_5 ΣHC)	0 01	0 004
(C_6 ΣHC)	0 004	0 002
Olefin paraffin ratio		
C_2	0 24	0 12
C_3	0 91	0 25
C_4	2 03	0 50
C_5	1 49	0 75

[a] Reaction conditions pressure = 10 bar, H_2 CO = 1 1, total flow rate = 20 cm^3/min

[b] Reaction rate r in mol of product (mol of Os s)$^{-1}$

[c] This set of data was obtained in an independent experiment to check reproducibility The data may be compared with those in line 2 of Table 2

ever, remained unaffected by the H_2 CO ratio at both pressures

The effect of the pretreatment conditions is illustrated in Table 3 These data indicate that the activity for hydrocarbon formation of the more severely reduced catalyst (pretreatment A) was markedly higher than that of the less severely reduced catalyst (pretreatment B) The effect on methane selectivity does not appear to be strong, C_2 selectivity is somewhat higher for pretreatment B, whereas C_3 through C_6 selectivities are higher for pretreatment A The olefin paraffin ratios are strongly dependent on the severity of the reduction, these ratios are lower for all carbon numbers from C_2 to C_5 after pretreatment B However, whereas after pretreatment A they have a maximum value at C_4 [as mentioned above (Table 2, Fig 5)], after pretreatment B they tend to increase continuously from C_2 to C_5

A comparison is made in Table 4 of the catalytic behavior for CO hydrogenation of three Al_2O_3-supported osmium catalysts which were prepared using different precursor compounds The conversions were roughly equal in the different experiments ($\lesssim$1%) The data of Table 4 show that the activity for CH_4 formation was lowest for the $[Os_3(CO)_{12}]$-derived catalyst and highest for the $[Os(CO)_5]$-derived catalyst after the (more severe) pretreatment A, while the activity of a $[H_2OsCl_6]$-derived catalyst was intermediate Moreover, the selectivity for methane formation was pronounced for the two catalysts derived from $[Os_3(CO)_{12}]$ and $[H_2OsCl_6]$, for which the amounts of C_2 and higher hydrocarbons were sharply less The $[Os(CO)_5]$-A catalyst gave lower yields of methane accompanied by significant amounts of higher hydrocarbons in the C_2–C_6 range

We emphasize that the $[Os_3(CO)_{12}]$- and $[H_2OsCl_6]$-derived catalysts did not show any detectable metal aggregation, either before or after their use as catalysts for extended periods (*3*) They were characterized by infrared spectroscopy and TEM and found to consist of ensembles of three (and in the case of $[H_2OsCl_6]$, perhaps less than three) mononuclear surface carbonyl

TABLE 4

Comparison of CO Hydrogenation on Various Al_2O_3-Supported Osmium Catalysts[a]

	Catalyst precursor		
	$[Os_3(CO)_{12}]$[b]	$[H_2OsCl_6]$[c]	$[Os(CO)_5]$ A
$10^4 r_{CH_4}$[d]	1 5	25	38 6
Selectivity			
(C_1 ΣHC)	0 81	0 95	0 52
(C_2 ΣHC)	0 16	0 047	0 25
(C_3 ΣHC)	0 03	0 002	0 15
(C_4 ΣHC)	—	—	0 05
(C_5 ΣHC)	—	—	0 02

[a] Reaction conditions total pressure = 1 bar H_2 CO = 3 1 reaction temperature = 606 K for $[Os_3(CO)_{12}]$ and $[H_2OsCl_6]$, and 598 K for $[Os(CO)_5]$-A

[b] Loading 0 34 wt% Os data from ref (*3*)

[c] Loading 1 18 wt% Os, data from ref (*3*)

[d] Reaction rate r in mol of product (mol of Os s)$^{-1}$

complexes (*3*) The significantly higher yield of hydrocarbons with carbon number >2 for the $[Os(CO)_5]$-derived samples indicates a higher probability for chain propagation on these catalysts

This result suggests that metal aggregation occurred under the relatively severe pretreatment conditions (namely, the high partial pressure of H_2) applied in the present investigation This expectation is supported by the physical characterization of the used catalysts, as shown in the following section

Characterization of Used Catalysts

The used catalysts were characterized by TEM and infrared spectroscopy The electron micrographs of the catalysts after pretreatment conditions B and A are shown in Figs 2c and d, respectively These micrographs appear to be slightly diffuse, making difficult an exact determination of particle sizes This difficulty arises from charging effects and the resulting drifts of particles in the specimen brought about by the relatively high current densities required for an instrumental magnification of 360,000× In some experiments, therefore, a carbon film with an approximate thickness of 4 nm was evaporated onto the specimens This film had the effect of preserving structure and reducing the charging phenomena without influencing the resolution Particle size determinations could be done much more accurately with these samples

The catalyst $[Os(CO)_5]$-B, pretreated with 1 bar of H_2 for 1 h prior to its use in the CO + H_2 reaction, contained only very few aggregates, with a maximum size of 1 7 nm (Fig 2c) We infer that most of the osmium was still present as mononuclear species or aggregates too small for detection by TEM (<1 nm) in these samples This interpretation is confirmed by the infrared spectra of the used catalyst—which were nearly identical to spectra of the unused samples The spectra suggest the presence of surface osmium carbonyl complexes with the metal in various oxidation states Small contributions from CO adsorbed on the aggregates were probably overwhelmed by the carbonyl bands of the complexes and, hence, escaped detection

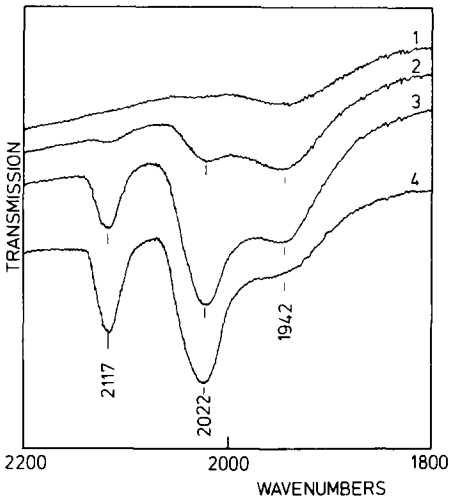

FIG 6 Infrared spectra of a used catalyst $[Os(CO)_5]$-A (1) after evacuation at 300 K for 18 h, (2) after adsorption of CO (0 13 bar) for a few minutes at beam temperature, (3) after subsequent exposure to CO at 530 K for 3 5 h, and (4) at 605 K for 5 2 h

In contrast, the micrographs of the used catalyst $[Os(CO)_5]$-A, pretreated under the relatively severe conditions, showed appreciable aggregation, with an upper limit of Os particle diameters of 2 5 nm (Fig 2d) This sample did not show any strong absorption in the carbonyl stretching region before exposure to CO (Fig 6, spectrum 1) However, exposure to 1 3 × 10^2 mbar of CO at the beam temperature (approximately 370 K) for a few minutes produced two broad carbonyl bands near 2020 and 1940 cm^{-1} In agreement with the TEM results, these bands are indicative of CO chemisorbed on osmium metal particles This assignment follows from the nearly identical carbonyl spectra obtained for CO chemisorbed on a conventionally prepared 5-wt%-Os/Al_2O_3 sample made from $[H_2OsCl_6]$ and reduced in H_2, which contained osmium particles in the size range ~0 5 to 4 nm (*26*) Exposure of the sample to a CO atmosphere at higher temperatures

led to the progressive formation of a new band at 2117 cm^{-1} and an increase in intensity of the band at 2022 cm^{-1} (Fig 6, spectra 3 and 4) These spectra closely resemble those of the fresh catalysts in CO atmospheres and suggest the formation of mononuclear tricarbonyl species, the spectra of which obscure those of CO chemisorbed on aggregates These complexes may be produced by carbonylation (and oxidation) of some isolated osmium atoms or by disintegration of small aggregates (or dissociation of edge atoms from larger aggregates) as a result of the reaction with CO

We conclude from the TEM and infrared characterizations of the used catalysts that aggregation was significantly more pronounced for the severe pretreatment A than for the mild pretreatment B, confirming the inference from the product distributions observed in the CO + H_2 reaction

Catalyst Structure and Reaction Mechanism

In summary, the data show that osmium catalysts derived from various precursor complexes are active for the CO + H_2 reaction, with the activity being strongly dependent on the structure of the osmium species The activities of the catalysts containing mononuclear osmium complexes {derived from $[Os_3(CO)_{12}]$ and $[H_2OsCl_6]$} are lower than those in which reduction had occurred {$[Os(CO)_5]$-A and $[Os(CO)_5]$-B} (Table 4) Moreover, the more strongly reduced and aggregated catalyst $[Os(CO)_5]$-A is slightly more active than $[Os(CO)_5]$-B (Table 3) We emphasize that rates were calculated on the basis of total Os in the catalyst, rates normalized to surface Os would show more pronounced differences

These observations may be tentatively explained as follows If the active species can indeed be a mononuclear complex, CO activation may occur with the assistance of a surface Lewis acid site, Al^{3+}_{cus}, as proposed previously (*7–10*)

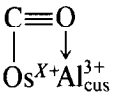

Driessen *et al* (*35*) have recently shown that a Pd/SiO_2 catalyst, which contained Pd^{n+} ions produced methanol with high selectivity, a behavior which markedly differs from that of the present Os/Al_2O_3 catalysts An explanation for the different selectivities may possibly be found in the negligible Lewis acidity of silica

The higher activities of the reduced and aggregated Os samples may be explained as follows CO activation may occur analogously, with CO being coordinated to edge atoms of aggregates at the interface with the support as suggested by Burch and Flambard (*27*) and by Shriver (*8*)

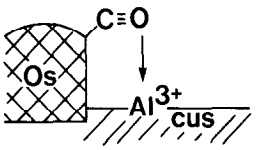

The higher rates observed with these catalysts compared with those containing isolated cationic Os species may be a consequence of the lower oxidation state of the Os edge atom, which would lead to a more pronounced backbonding

The possibly expected low frequency carbonyl infrared bands for such species could not be detected This failure, however, does not necessarily rule out this type of interaction since low concentrations of such intermediates would not permit their infrared detection

Alternatively, CO may dissociate on adjacent Os metal atoms of the aggregates

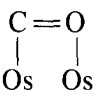

A distinction between these two possibilities cannot be made on the basis of the present results

The methanation rate measured for the strongly reduced and aggregated catalyst $[Os(CO)_5]$-A at 1 bar 598 K and an H_2 CO

ratio of 3 was 8.9×10^{-4} mol (mol of Os s)$^{-1}$ (Table 2) This value (recall that it represents a value less than the turnover frequency) may be compared with the turnover frequencies reported by Vannice (*28*) for other group VIII metals supported on Al_2O_3 The activities decreased in the sequence Ru $\gg$ Ni > Co > Rh $\approx$ Pd $\gg$ Pt > Ir, where the least active metal Ir had a turnover frequency of 1.8×10^{-3} s^{-1} A comparison with the data for $[Os(CO)_5]$-A suggests that Os should be classified among the least active metals in this series—which would be in agreement with Vannice's correlation of turnover frequencies with heats of adsorption of CO (*29*) if a rather high heat of adsorption of CO on Os metal were appropriate This value has not been measured, we note, however, that the average Os–CO bond energy in $[Os_3(CO)_{12}]$ is large, 190 kJ mol^{-1} (*30*)

An effect of Os structure is also manifested in the product distributions The catalysts presumed to contain the mononuclear Os species gave predominantly methane, whereas higher hydrocarbons were produced in higher yields with the reduced and aggregated catalysts Moreover, the larger aggregates of $[Os(CO)_5]$-A had greater selectivities for higher hydrocarbons (Table 3) Such particle size effects on product chain length have been described and explained previously by Nijs and Jacobs (*7, 31*)

Olefin paraffin ratios were also found to be dependent on the H_2 CO ratio and the degree of metal aggregation (Fig 5, Table 3) $[Os(CO)_5]$-B gave lower olefin paraffin ratios than $[Os(CO)_5]$-A for all carbon numbers, and olefin paraffin ratios passed through a maximum at C_3 or C_4 for catalyst $[Os(CO)_5]$-A Olefin paraffin ratios are expected to be determined by the relative probabilities of the alternate routes for chain termination (*32*), i e , β-hydrogen abstraction to yield olefins

$$(C_nH_{2n+1})_{ads} + s \rightarrow C_nH_{2n} + s + H_{ads} \quad (1)$$

and hydrogen addition to yield paraffins

$$(C_nH_{2n+1})_{ads} + H_{ads} \rightarrow C_nH_{2n+2} + 2s \quad (2)$$

The probability for step (1) depends on the density of open coordination sites s in the proximity of the growing chain and that for step (2) is determined by the density of hydrogen atoms adsorbed near the growing chain The surface of a particle under stationary catalytic reaction conditions at low conversions can be expected to be highly covered with CO_{ads} and C_{ads}, and hence the density of free sites and of adsorbed hydrogen atoms is expected to be low (*32*) The density of open sites may be particularly low on small aggregates, and steric hindrance to the approach of the β-hydrogen connected with longer chains may be less than on larger aggregates These two ideas provide a tentative explanation of the experimental results They might be of some value for the design of catalysts for synthesis of lower olefins from synthesis gas

ACKNOWLEDGMENTS

The work done in Munich was supported by the Deutsche Forschungsgemeinschaft and the Fonds der Chemischen Industrie, the work done in Delaware was supported by the National Science Foundation A NATO grant provided support for the joint research Y Z was a recipient of a grant from the German Academic Exchange Service We acknowledge the help of Prof B Bogdanovic in providing the facilities for the $[Os(CO)_5]$ synthesis

REFERENCES

1 Biloen, P , and Sachtler, W M H , *Advan Catal* **30,** 165 (1981)
2 Ichikawa, M , *Bull Soc Chem Soc Japan* **51,** 2273 (1978)
3 Knozinger, H , Zhao, Y , Tesche, B , Barth, R , Epstein, R , Gates, B C , and Scott J P , *Faraday Disc Chem Soc* **72,** 53 (1981)
4 Muetterties, E L , and Stein, J *Chem Rev* **79,** 479 (1979)
5 Nijs, H H , and Jacobs, P A , *J Catal* **65,** 328 (1980)
6 Hugues, F , Besson, B , and Basset, J -M , *J Chem Soc Chem Commun* 719 (1980)
7 Knozinger, H , Zhao, Y , Gates, B C , Scott, J P , and Tesche, B , Proc 3rd All-Union Conf "Mechanism of Catalytic Reactions," Novosibirsk (USSR), April, 1982, in press

8 Shriver, D F , *ACS Symp Ser* **152,** 1 (1981)
9 Brown, T L , *J Mol Catal* **12,** 41 (1981)
10 Burch, R , and Flambard, A R , *J Chem Soc Chem Commun* 123, (1981), *React Kinet Catal Lett* **17,** 23 (1981)
11 Guglielminotti, E , *J Mol Catal* **13,** 207 (1981)
12 Kazusaka, A , and Howe, R , *J Mol Catal* **9,** 183 (1980)
13 Laniecki, M , and Burwell, R L Jr *J Colloid Interface Sci* **75,** 95 (1980)
14 Brenner, A , and Hucul, D A , *J Amer Chem Soc* **102,** 2484 (1980)
15 Hieber, W , and Stallmann, H , *Z Elektrochem* **49,** 288 (1943)
16 Calderazzo, F , and Leplattenier, F , *Inorg Chem* **6,** 1220 (1967)
17 Knozinger, H , Stolz, H , Buhl, H , Clement, G , and Meye, W , *Chem Ing Tech* **42,** 548 (1970), and Knozinger, H , *Acta Cient Venez* **24,** Suppl 2 76 (1973)
18 Deeba, M , and Gates, B C , *J Catal* **67,** 303 (1981)
19 McQuade, K J , Scott, J P , Barth, R , Baek, K H , and Gates, B C , *Ind Eng Chem Fundam* submitted
20 Knozinger, H and Zhao, Y *J Catal* **71,** 337 (1981)
21 Smith, A K , Besson, B , Basset, J M , Psaro, R , Fusi, A , and Ugo, R , *J Organomet Chem* **192,** C31 (1980)
22 Besson, B , Moraweck, B , Smith A K , Basset J M , Psaro, R , Fusi, A , and Ugo, R , *J Chem Soc Chem Commun* 569 (1980)
23 Shvets, V A , Tarasov, A L , Kazansky, V B , and Knozinger, H , *J Catal* , in press
24 Schwank J , Allard L F , Deeba M and Gates B C *J Catal* **84,** 27 (1983)
25 Tesche, B , Zeitler, E Alizo Delgado, E , and Knozinger, H , Proc 40th Ann EMSA Meeting, Washington 1982, p 658
26 Kunzmann, G , Ertl, G , Knozinger, H , and Tesche, B unpublished
27 Burch, R , and Flambard, A R , *in* ' Metal-Support and Metal-Additive Effects in Catalysis' (B Imelik *et al* Eds), p 193 Elsevier, Amsterdam 1982, *J Catal* **78,** 389 (1982)
28 Vannice, M A , *J Catal* **37,** 462 (1975)
29 Vannice, M A , *J Catal* **50,** 228 (1977)
30 Muetterties, E L , Rhodin, T N , Band, E , Brucker, C F , and Pretzer W R , *Chem Rev* **79,** 91 (1979)
31 Nijs, H H and Jacobs, P A *J Catal* **66,** 401 (1980)
32 Sachtler, W M H , *Chem Ing -Tech* **54,** 901 (1982)
33 Collier, G Hung, D J , Jackson, S D , Moyes, R B , Pickering, J A , Wells, P B Simpson, A F , and Whyman, R , *J Catal* **80,** 154 (1983)
34 Knozinger, H , *Angew Chem* **80,** 778 (1968) *Angew Chem Int Ed* **7,** 791 (1968)
35 Driessen J M , Poels, E K , Hindermann, J P , and Ponec, V , *J Catal* **82,** 26 (1983)